Websites:
http://www.sciencepub.net/academia
http://www.sciencepub.net

Emails:
aarena@gmail.com
editor@sciencepub.net

Academia Arena

MARSLAND PRESS
Multidisciplinary Academic Journal Publisher

Significance of activation energy and nonlinear thermal radiation in a reactive micropolar nanofluid flow model over a stretching sheet with weak concentration

*A. Nwagwo, O.A. Esan, O.E. Enobabor, T.O. Ogunbayo, O.M. Ayeni, B.O. Olusan

Department of Mathematics, Yaba College of Technology, Yaba, Nigeria.
*naxander2000@yahoo.com, *alexander.nwagwo@yabatech.edu.ng

Abstract
A two dimensional vertically stretching sheet is configured in this study. There is a flow of a non-Newtonian electro-conducting reactive micropolar nanofluid over this device with the influence of activation energy, Brownian movement of tiny particles, thermo-migration of particles and nonlinear thermal radiation. By means of suitable similarity variables, the partial derivatives governing the flow equations are remodeled into ordinary derivatives and afterward solved by using a numerical approach via Runge-Kutta Fehlberg method. The consequences of this study reveal that the micropolar fluid has the tendency to boost the velocity profiles whereas there is a depletion of the momentum boundary layer with higher magnitudes of the magnetic field term. There is a reduction in the nanoparticles concentration profiles with higher values of chemical reaction and Brownian motion whereas the presence of activation energy and thermophoresis term raises the concentration field.
[A. Nwagwo, O.A. Esan, O.E. Enobabor, T.O. Ogunbayo, O.M. Ayeni, B.O. Olusan. **Significance of activ ation energy and nonlinear thermal radiation in a reactive micropolar nanofluid flow model over a st retching sheet with weak concentration.** *Academ Arena* 2023;15(7):1-10]. ISSN 1553-992X (print); ISSN 2158-771X (online). http://www.sciencepub.net/academia. 01.doi:10.7537/marsaaj150723.01.

Keywords: Micropolar fluid, Activation energy; Brownian motion; Thermophoresis.

1 Introduction

The origin of the theory of micropolar fluid is traceable to the work of Eringen (1966) with that of thermo-micropolar by same author in (1972). This fluid is categorized as a non-Newtonian fluid with microstructures and anti-symmetric stress tensor. It is a class of complex fluid with spinning tendency and characterizes microscopic influence due to the intrinsic microstructural arrangements of the fluid elements (Lukaszewicz, 1999; Reena and Rana, 2009). The various particles in micropolar fluid are of varying sizes and manifest expanding of shrinking attributes and capable of of rotation individually. Micropolar fluid has been found to be appropriate for the simulation of some complex fluids like polymeric additives, blood, colloidal suspensions, liquid crystals, etc of which the Navier-Stokes concept cannot predict accurately.
The term nanofluid explains those fluids with minutes nanoparticles such as metals, oxides, carbides, etc. This new class of fluids aids thermal conductivity and heat transfer as compared with the regular heat transfer fluids like water, oil, ethylene glycol, etc. In various industrial and engineering operations, such as in power manufacturing and atomic reactors, heating and cooling are often encountered. Nanofluids have the capacity to enhance cooling process in high-energy equipment. The blend of the micropolar fluid with tiny nanoparticles is significant in diverse fields of engineering, manufacturing, science and technology. For instance, in bio-medical engineering like fluid flow in brains and blood flows; metallurgical drawing of filaments, chemical engineering including paint rheology; drug production, etc. On the ground of these crucial applications, various researchers have shown interest in such investigations. For instance, Akbar *et al.* (2013) evaluated the flow of hydromagnetic-nanofluid near a stagnation point alongside with radiation and conditioned by a convective surface heating while Noor *et al.* (2015) numerically reported such a study using micropolar nanofluid over a vertically stretched surface with slip properties.
The flow of fluids near the bounding surface and generated by expanding materials has received huge attention from researchers owing to the importance in industrial and engineering operations. For instance, hot rolling, wire drawing, the extrusion of polymer and plastic sheet, paper and textile production,etc. Rising from the work of Crane (1970), there has been a numerous extension of such a concept on diverse configurations, thermal conditions and flow assumptions (see Kumar, 2009; Makinde and Aziz, 2011; Akinbobola and Okoya, 2015; Fatunmbi and Fenuga, 2018). Many engineering and material manufacturing processes generate high temperature, for instance, in nuclear power plants, hot rolling, heat

exchangers, electrical power generation and so on. In such processes, the knowledge of thermal radiation becomes crucial for the construction of relevant devices including energy conversion gadgets. The modelling of the radiative heat flux can be linear or nonlinear types depending on the intensity of temperature difference in the flow region. The linear case can be considered valid when there is low temperature difference whereas the nonlinear type is appropriate for situations of low and high temperature differences. However, for accurate prediction and wider applications of thermal radiation, the nonlinear type is considered in the present study as incorporated by Parida *et al.* (2015), Gbadeyan et al. (2020); Fatunmbi and Adeniyan (2020). Chemical reaction can be classified as homogeneous or heterogeneous operations. In well-mixed systems, when all the reactants occur in the same phase, the reaction is said to be homogeneous, for instance, a reaction that takes place between two gases or two liquids or two solids. Also, the term activation energy is a description of least amount of energy required for chemical reaction to occur. In other words, the minimum magnitude of energy needed to transform the species that change the reactants into products. In the presence of activation energy, there is rapid flow of particles. Due to its importance, various scholars have reported on such a phenomenon in the recent time. Ramzan *et al.* (2018) developed a mathematical model for the micropolar fluid flow with activation energy coupled with chemical reaction and nonlinear thermal radiation, Khan *et al.* (2018) studied such a concept on the stagnation point flow impacted by buoyancy forces while Kumar *et al.* (2018) applied Carreau fluid with the influence of Cattaneo-Christov condition to report such a phenomenon.

The main goal of the current analysis is to investigate the impact of activation energy, nonlinear thermal radiation and other physical parameters on the flow, heat-mass transfer of an electrically conducting micropolar nanofluid configured in a two-dimensional vertically stretched surface. The model also characterizes the inclusion of thermophoresis, Brownian motion, chemical reaction with prescribed surface temperature condition as the thermal heating condition. In therms of applications, this work is essentially applicable in engineering and industrial processes including pharmaceutical operations, industrial cooling, transportation industries, cooling of electronic components, etc. Various graphs are drawn to showcase the reaction of the various physical parameters on the dimensionless quantities for better prediction.

The rest of the work is organized as fellows: the next section deals with the problem development and analysis(the govering equations, notations and transformed equations). In section 3, we consider the method of solutions while section 4 deals with the analysis of the results and discussion. The last section is a brief conclusion.

2 Problem Development and Analysis

A two-dimensional, time-independent, incompressible motion of an electro-conducting micropolar nanofluid is developed in this work. The fluid motion is assumed to be in the upward route towards x direction. A perpendicular direction to the flow route is y axis and the imposed magnetic field. The geometry of flow is coordinated by x, y coordinates having velocities u and v respectively as described in figure 1. The surface velocity is taken as $u = u_w = ax$ where $a > 0$ indicates stretching rate whereas velocity upstream is assumed to be zero. Ignoring the induced magnetic field influence on the account of low magnetic Reynolds number. An assumption that the thermal field has a large temperature difference within the flow is applied and as such, the usage of the nonlinear Rosseland approximation is valid. The fluid properties are supposed to be isotropic and constant apart from the density variation in the body force term in the momentum equation which is approximated by Oberbeck-Boussinesq approximation. The presence of thermophoresis, Brownian motion, first order chemical reaction and activation energy are also incorporated in the flow region.

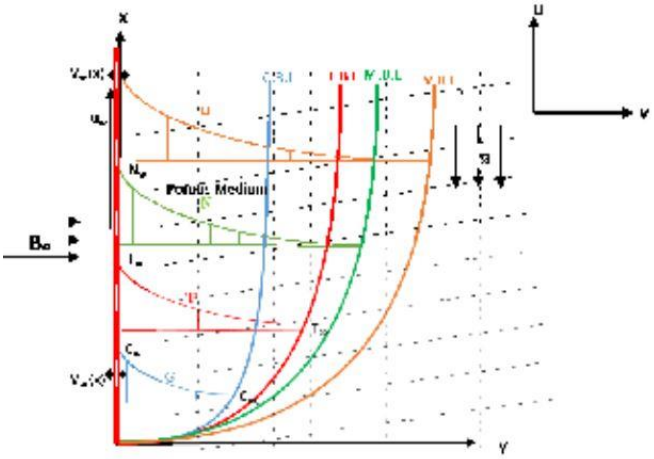

Fig. 1 Flow Geometry

2.1 The Governing Equations

The governing equations have been derived following the assumptions in the section above. Then Oberbeck-Boussinesq and boundary layer approximations are also applied to formulate the relevant equations as listed below.

Academia Arena
Websites:
http://www.sciencepub.net/academia
http://www.sciencepub.net
Emails:
aarena@gmail.com
editor@sciencepub.net
MARSLAND PRESS
Multidisciplinary Academic Journal Publisher

$$\frac{\partial u}{\partial x} = -\frac{\partial v}{\partial y}, \tag{1}$$

$$\rho\left(u\frac{\partial u}{\partial x} + v\frac{\partial u}{\partial y}\right) - (\mu + r)\frac{\partial^2 u}{\partial y^2} = \mu\frac{\partial G}{\partial y} + g\beta_T(T - T_\infty) + g\beta_C(C - C_\infty) - \sigma B_0^2, \tag{2}$$

$$u\frac{\partial T}{\partial x} + v\frac{\partial T}{\partial y} - \frac{k_f}{(\rho c_p)_f}\frac{\partial^2 T}{\partial y^2} = \frac{(\rho c_p)_p}{(\rho c_p)_f}\left(\frac{\partial T}{\partial y}\right)\left[\frac{D_T}{T_\infty}\left(\frac{\partial T}{\partial y}\right) + D_B\left(\frac{\partial T}{\partial y}\frac{\partial C}{\partial y}\right)\right] + \frac{(\mu+r)}{(\rho c_p)_f}\left(\frac{\partial u}{\partial y}\right)^2 + \frac{\sigma B_0^2}{(\rho c_p)_f}u^2 + \frac{1}{(\rho c_p)_f}\frac{16\sigma^\star}{3k^\star}\left(T^3\frac{\partial^2 T}{\partial y^2} + 3T^2\left(\frac{\partial T}{\partial y}\right)^2\right), \tag{3}$$

$$u\frac{\partial G}{\partial x} + v\frac{\partial G}{\partial y} - \frac{\gamma}{\rho_f j}\frac{\partial^2 G}{\partial y^2} = -\frac{\mu}{\rho j}\left(2G + \frac{\partial u}{\partial y}\right), \tag{4}$$

$$u\frac{\partial C}{\partial x} + v\frac{\partial C}{\partial y} = D_b\frac{\partial C^2}{\partial y^2} + \frac{D_t}{T_\infty}\left(\frac{\partial^2 T}{\partial y^2}\right) - k_r^2(C - C_\infty)\left(\frac{T}{T_\infty}\right)^n \exp\left(-\frac{E_0}{\beta T}\right). \tag{5}$$

The associated boundary conditions for the governing equations are:

$$u = u_w = ax, v = 0, G = -s\frac{\partial u}{\partial y}, T = T_w = (T_\infty + Ax^\kappa), C = C_w aty = 0,$$
$$u \to 0, G \to 0, T \longrightarrow T_\infty, C \longrightarrow C_\infty, \quad as \;\; y \to \infty. \tag{6}$$

2.2. Notations

All symbols featuring in the above equations are: T (Temperature), ν_f (kinematic viscosity), C (concentration of of nanoparticles), ρ_f (density), s (surface boundary parameter), r (vortex viscosity), g (acceleration due gravity), σ (electrical conductivity), j (micro inertia density), $(\rho c_p)_f$ (heat capacity of the fluid), γ (spin gradient viscosity), k_f (thermal conductivity), T_∞ (temperature at free stream), C_∞ (concentration at the free stream), (ρ_p) (nanoparticle density), E_0 (activation energy), $(\rho c_p)_f$ (heat capacity of nanoparticle), k_r (chemical reaction rate), D_b (Brownian diffusion coefficient), D_t (thermophoretic diffusion coefficient), a (stretching rate), n (fitted rate constant), μ (dynamic viscosity), G (microrotation component). The micropolar surface boundary parameter s in this study is assumed to be $s = 0.5$ which implies weak concentration of the micro-elements at the wall surface.

2.3 Transformed Equations

By incorporating the similarity variables and the non-dimensional quantities in Eq. (7), the main equations are appropriately re-modelled from partial into ordinary derivatives.

$$\frac{\eta}{y} = \sqrt{\frac{a}{\nu_f}}, \frac{\psi}{f(\eta)} = \sqrt{a\nu_f}x, \frac{G}{ag(\eta)} = \sqrt{\frac{a}{\nu_f}}x, \gamma = \left(\mu + \frac{r}{2}\right)j,$$
$$\theta(\eta) = \frac{T - T_\infty}{T_w - T_\infty}, \phi(\eta) = \frac{C - C_\infty}{C_w - C_\infty}, j = \frac{\nu_f}{a}. \tag{7}$$

Hence, on substituting quantities (7) into the governing equations, the validity of Eq. (1) is assured while Eqs. (2-5) result to the underlisted ordinary derivatives with respect to η:

$$(1 + K)f''' + ff'' - f'^2 + Kg' - Mf' + \lambda_1\theta + \lambda_2\phi = 0, \tag{8}$$

$$[1 + Nr(1 + (\theta_r - 1)\theta)^3]\theta'' + 3Nr(\theta_r - 1)\theta'^2(1 + (\theta_r - 1)\theta)^2 + PrEcMf'^2 + Pr(f\theta' - \kappa f'\theta) + (1 + K)Ecf''^2 + Pr(Nt\theta'^2 + Nb\theta'\phi') = 0, \tag{9}$$

$$(1 + K/2)g'' + fg' - f'g - K(2g + f'') = 0, \tag{10}$$

$$\phi'' + Scf\phi' - Sc\gamma_1(1 + \xi\theta)^n exp\left(-\frac{E}{1+\xi\theta}\right)\phi + \frac{Nt}{Nb}\theta'' = 0. \tag{11}$$

subject to:

$$\begin{aligned} at \quad & \eta = 0: f'(\eta) = 1, f(\eta) = 0, g(\eta) = -hf'', \theta(\eta) = 1, \phi(\eta) = 1 \\ as \quad & \eta \to \infty: f'(\eta) = 0 \;\; g(\eta) = 0, \theta(\eta) = 0, \phi(\eta) = 0. \end{aligned} \tag{12}$$

Where

$$\begin{aligned} & \theta_r = \frac{T_w}{T_\infty}, \xi = \frac{(T_w - T_\infty)}{T_\infty}, K = \frac{r}{\mu}, Pr = \frac{\mu c_p}{k_f}, M = \frac{\sigma B_0^2}{a\rho}, Nr = \frac{16\sigma^\star T_\infty^3}{3k^\star k_\infty} \\ & Ec = \frac{u_w^2}{c_p(T_w - T_\infty)}, \lambda_1 = \frac{Gr_x}{Re_x}, \lambda_2 = \frac{Gc_x}{Re_x}, Sc = \frac{\nu_f}{D_B}, \gamma_1 = \frac{k_r^2}{m}, E = \frac{E_0}{\beta T_\infty}, Nt = \frac{D_T \tau (T_w - T_\infty)}{T_\infty \nu_f} \\ & Nb = \frac{D_B \tau (C_w - C_\infty)}{\nu_f}. \end{aligned} \tag{13}$$

Where $\tau = \frac{(\rho c_p)_p}{(\rho c_p)_f}$ and $Gr_x = \frac{g\beta_T (T_w - T_\infty)}{a^2 x}$. The physical parameters listed in equation (13) above are temperature ratio, temperature relative term, material term, Prandtl number, magnetic field term, radiation parameter, Eckert number, thermal buoyancy, concentration buoyancy, Schmidt number, chemical reaction term, activation energy, thermophoresis term and brownian motion respectively.

Likewise, the corresponding quantities of engineering delight are skin frictional factor, local Nusselt number and Sherwood number as orderly presented in equation (14).

$$C_{fx} = \frac{s_w}{\rho_f u_w^2}, Nu_x = \frac{x h_w}{k(T_w - T_\infty)}, Sh_x = \frac{x t_m}{D_b(C_w - C_\infty)}. \tag{14}$$

The non-dimensional forms of these quantities are

$$C_{fx} = [1 + (1 - s)K] Re_x^{-1/2} f''(\eta) \quad at \quad \eta = 0, \tag{15}$$

$$Nu_x = -[1 + Nr(1 + (\theta_r - 1)\theta(\eta))^3] Re_x^{1/2} \theta'(\eta) \quad at \quad \eta = 0, \tag{16}$$

$$Sh_x = -Re_x^{1/2} \phi'(\eta) \quad at \quad \eta = 0. \tag{17}$$

where $s_w = \left[(\mu + r)\frac{\partial u}{\partial y} + \mu G\right]_{y=0}$, $h_w = -\left[\left(k_f + \frac{16T^3\sigma^\star}{3k^\star}\right)\frac{\partial T}{\partial y}\right]_{y=0}$ and $t_m = -D_b\left(\frac{\partial C}{\partial y}\right)_{y=0}$ are shear stress, heat flux and mass flux respectively.

3 Method of solution

The solution to the system of equations (8-11) subject to equation (12) is obtained with a numerical approach due to the non-linearity of the governing equations. The numerical approach is sought through a popular shooting technique together with the scheme of Runge-Kutta-Fehlberg. For comprehensive details of this method, readers can check Ali (1994); Attili and Syam (2008); Mahanthesh et al. (2018). The default values for the computations are carefully chosen from the existing related works in literature as follows: $K = M = s = 0.5, Nt = Nb = 0.2, \theta_r = 1.3, Da = Rd = 0.3, \lambda_1 = \lambda_2 = 0.6, Sc = 0.44, \kappa = 0.5$ and $Pr = 0.72$ unless stated in the graphs. Table 1 gives the validation of the results gotten in this study with respect to Nu_x as compared with published works in the limiting constraints. In this comparison, the values of Pr and κ are varying while other parameters are zero. It is found that there exists a good agreement between the current work and the published items.

Table 1: Data for Nu_x for varying Pr and κ in comparison with published data

κ	Grubka and Bobba (1985)		current work	
	Pr =0.72	Pr = 1.0	Pr =0.72	Pr = 1.0
- 2.0	0.7200	1.0000	0.72069	0.99945
- 1.0	0.0000	0.0000	-0.00110	0.00012
0.0	-0.4631	-0.5820	-0.46359	-0.58201
1.0	-0.8086	-1.0000	-0.80883	-1.00001
2.0	-1.0885	-1.3333	-1.08862	-1.33333
3.0	-1.3270	-1.6154	-1.32707	-1.61538

4 Analysis of results and discussion

To make appropriate prediction based on the behaviour of the emerging parameters on the flow region, various graphs are constructed for velocity, temperature, microrotation and concentration under this section. There is an elevation in the velocity profiles due to a growth in the values of K as illustrated in figure 2. This trend is traceable to the fall in the dynamic viscosity by a rise in K. In the same manner, the microrotation field also advances by rising values of K as depicted in figure 3. Conversely, there is a depletion of the thermal field by higher values of K as portrayed in figure 4.

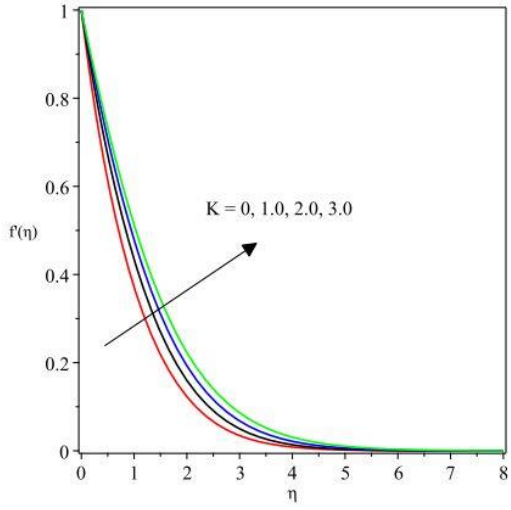

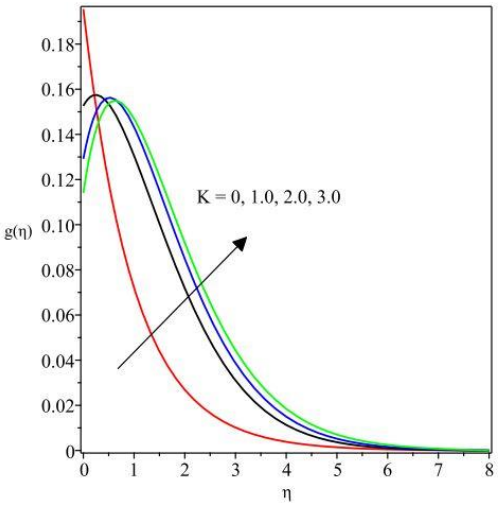

Fig. 2 velocity field versus K **Fig. 3** microrotation profiles versus K

Further, the implication of the magnetic field term M on the flow field is narrated in figure 5. Here, a rise in M depletes the fluid movement due to the action of the Lorentz force. This force is a kind of resistive force which enables the fluid motion to drag due to its interaction with the electro-conducting nature of the working fluid. The converse is true for the microrotation profile in that there exists an enhancement in the field of microrotation due to escalating M as found in figure 6. Likewise, the thermal region is enhanced due to higher M because of the additional heat generated by the resistance to the motion of the fluid induced by the Lorentz force as depicted in figure 7.

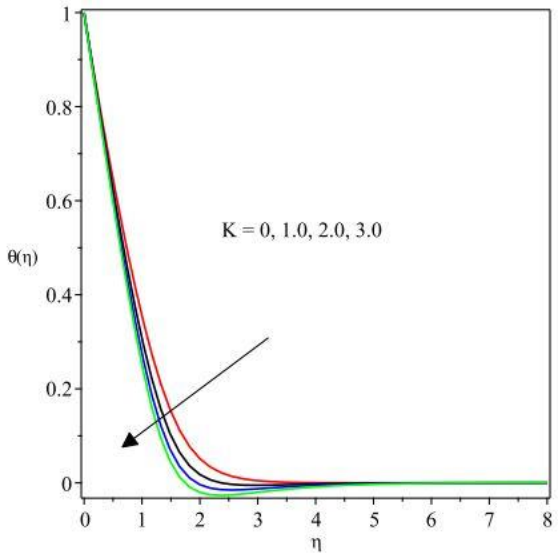

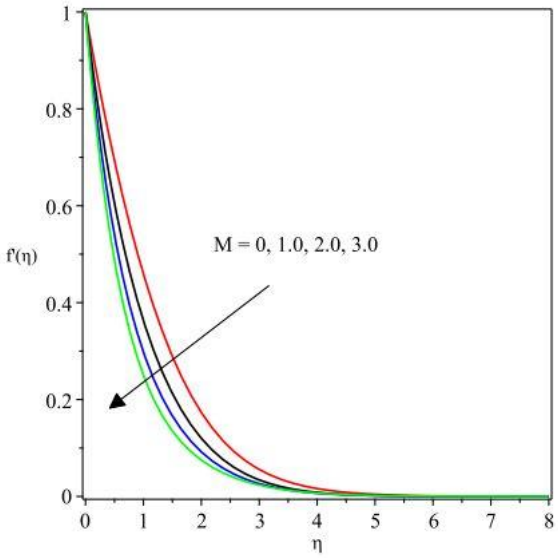

Fig. 4 temperature profiles versus K **Fig. 5** velocity profiles versus M

Figures 6 and 7 respectively describe the effects of the thermal buoyancy parameter λ_1 and the corresponding concentration buoyancy parameter λ_2 on the velocity filed. A boost in λ_1 dictates a higher buoyancy force over the viscous force. This buoyancy force acts favourably to the growth in the velocity profile as found in Fig. 6. In addition, this trend occurs due to the fact that vertical flows tend to improve with the growth in buoyancy force since λ_1 behaves as a favourable pressure gradient for such flows. In the like manner, the concentration buoyancy parameter λ_2 behaves in a similar on the velocity field as depicted in figure 7.

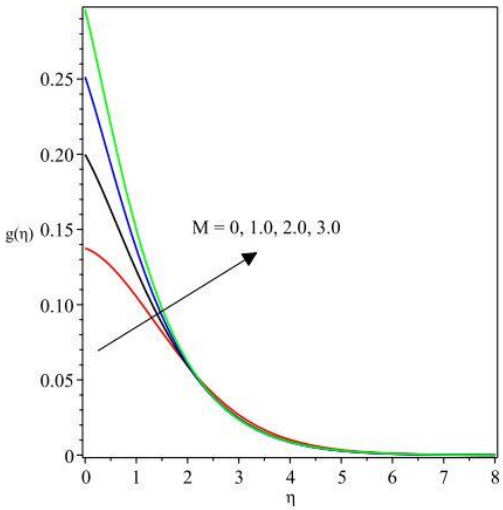

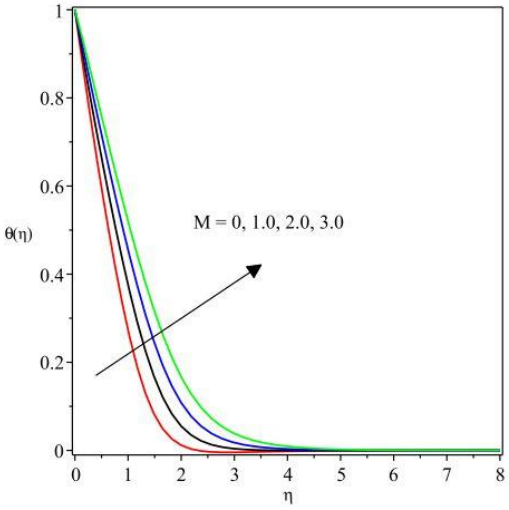

Fig. 6 microrotation profiles versus M **Fig. 7** temperature profiles versus M

Figure 8 and 9 orderly describe the reaction of λ_1 and λ_2 on the velocity distribution. In clear terms both terms raise the speed of the fluid. This pattern is possible due to the domineering nature of the buoyancy force over that of viscous force as these parameters grow in magnitude. A rise in the buoyancy force encourages the fluid transport to advance as found in these figures. Meanwhile, the reactions of these parameters on the thermal and nanoparticles concentration profiles are shown to be reducing these profiles as seen in figures 10 and 11 respectively.

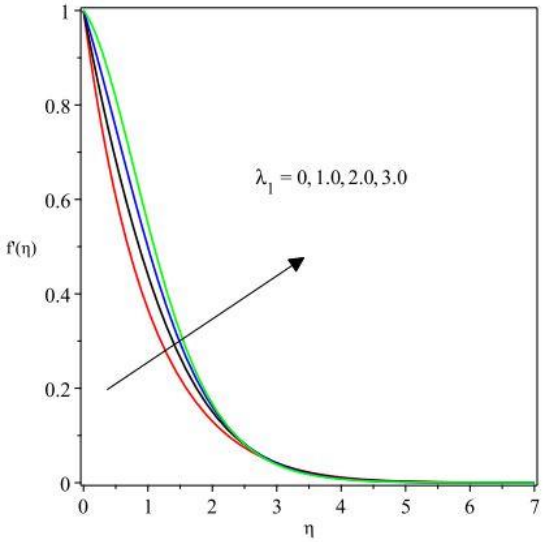

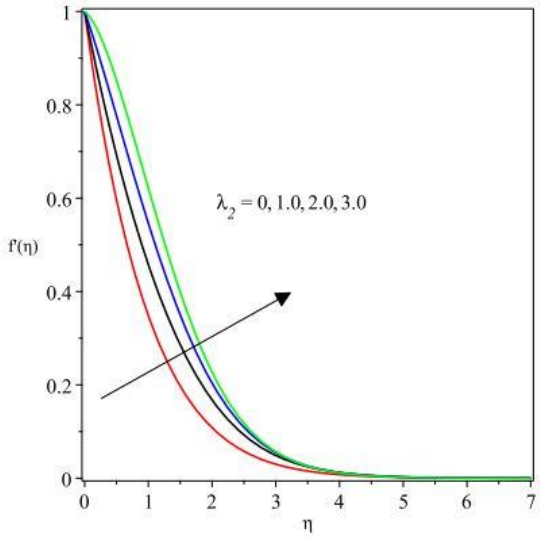

Fig. 8 velocity profiles profiles versus λ_1 **Fig. 9** velocity profiles profiles versus λ_2

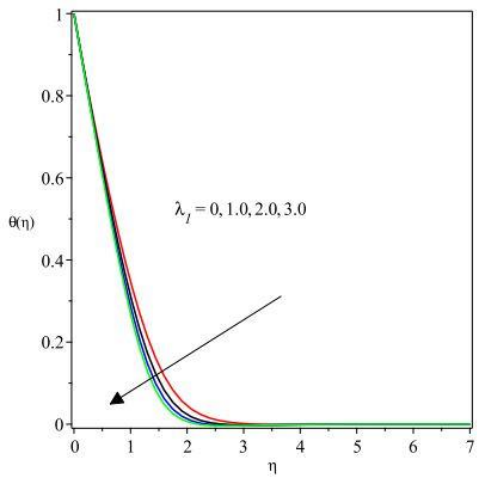

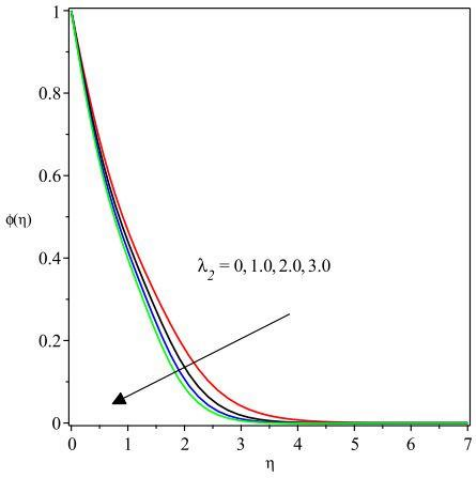

Fig. 10 temperature field versus λ_1**Fig. 11** concentration profiles versus λ_2

The parameter depicting the radiation parameter Nr is plotted against the heat region as demonstrated in figure 12. Evidently, the heat distribution rises by the advancement in Nr. There is a positive impact on the heat conduction due to a growth in Nr which in turn boost the temperature profile. In a similar way, augmentation of the temperature ratio term θ_r boosts the thermal field and create enhancement of the surface temperature as noticed in figure 13. The occurrence of such a reaction is attributed to the strength of the operating temperature $(T_w - T_\infty)$ which consequently favours the surface temperature.

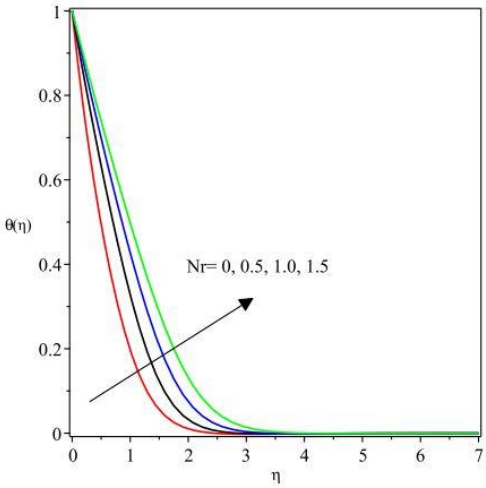

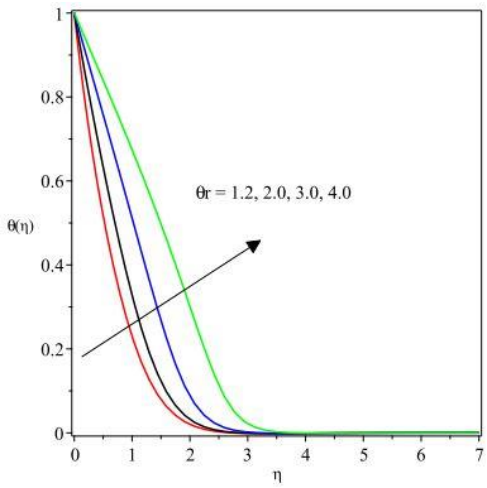

Fig. 12 temperature profiles versus Nr**Fig. 13** temperature field versus θ_r

The thermophoresis term Nt is found to raise both the surface temperature $\theta(\eta)$ and the concentration field $\phi(\eta)$ as displayed in figure 14 and 15. Thermophoresis force promotes a rise in the temperature profile due to the temperature gradient occasioned by the thermophoretic force. Such a force causes a higher flow further away from the sheet such that more heated fluid is drawn away from the sheet which consequently causes a rise in thermal field as Nt advances. The significant contribution of the Brownian motion quantity Nb on the temperature $\theta(\eta)$ and on the concentration region $\phi(\eta)$ are presented orderly in figures 16 and 17. Basically, the Brownian motion describes the irregular trend movement found in the nanoparticles by its suspension in the working fluid. By the virtue of the haphazard motion, there is an increase in the kinetic energy due to the enhanced motion of the fluid and thereby encourages a hike in the thermal profile.

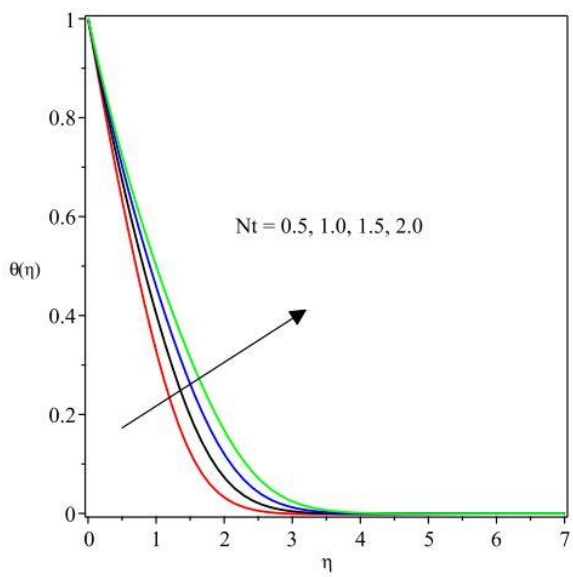

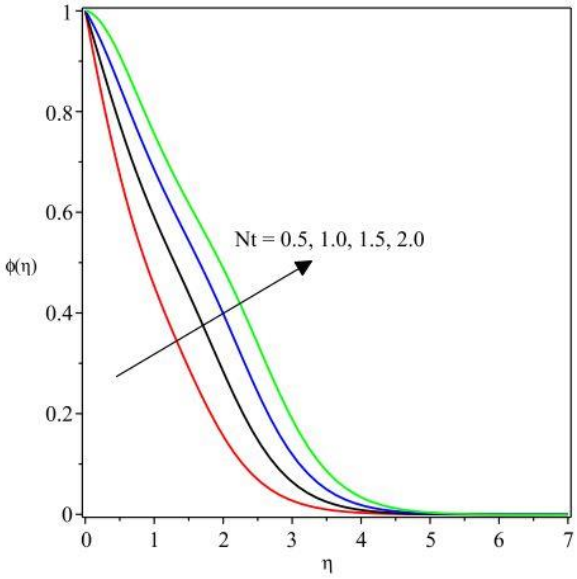

Fig. 14 temperature profiles versus Nt **Fig. 15** concentration profiles versus Nt

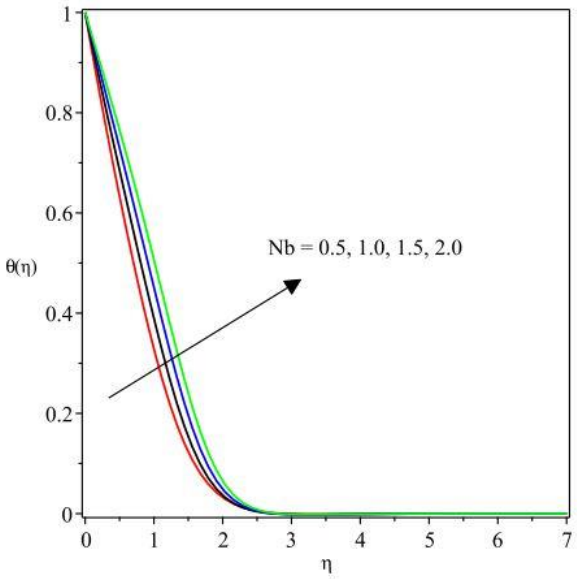

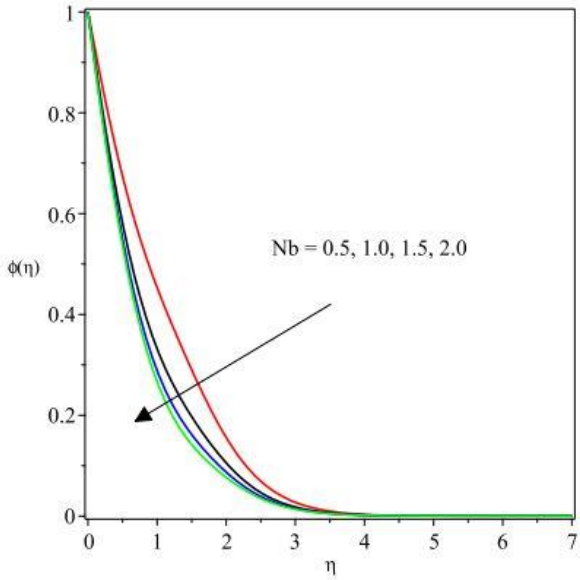

Fig. 16 temperature profiles versus Nb **Fig. 17** concentration profiles versus Nb

Figure 18 clearly reveals the behaviour of the concentration field to the variation in the activation energy term E. Evidently, escalating values of E propels a rise in concentration field. Higher rates of E causes the modified Arrhenius function to fall and encourages an increase in the generation of chemical reaction, thus, the concentration field is enlarged. However, such a pattern is reversed for a hike in the Sc as found in 19. This term describes the relative thickness of the momentum boundary layer to the mass diffusivity. Hence, a rise in Sc reduces the mass diffusivity and as such, there the concentration boundary layer thickness depreciates.

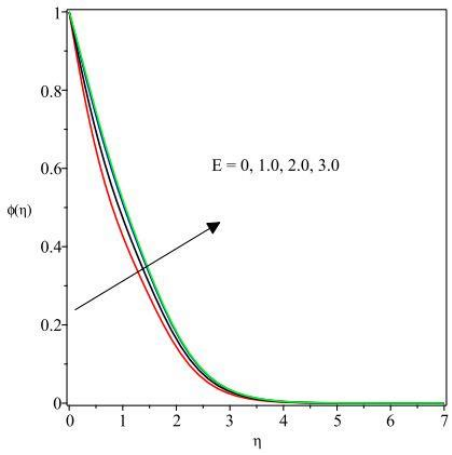

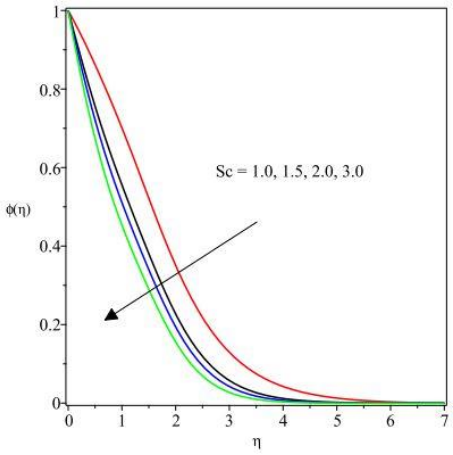

Fig. 18 concentration profiles versus E**Fig. 19** concentration profiles versus Sc

5 Conclusion

In the current work, an incompressible, steady two-dimensional flow of an electro-conducting micropolar nanofluid is investigated over an expanded sheet which stretches vertically upward. The model equation comprises of the activation energy, nonlinear thermal radiation, thermophoresis and Brownian motion effect coupled with prescribed surface temperature at the thermal boundary. The application of the similarity variables has been engaged to transform the governing equations to the ordinary forms from their former partial forms. Besides, the shooting technique is engaged as well as the Runge-Kutta Fehlberg scheme to provide the numerical solution due to the nonlinearity of the equations. The correctness of the solution is checked by comparing the surface heat propagation values with the published works in the limiting circumstances. The underlisted points summarize the main points drawn from this study.

•There is an acceleration in the velocity and microrotation profiles due to higher values of the material parameter K whereas the temperature field deletes with it.
• There is an expansion in the nanoparticle concentration boundary layer with enhancement in the values of the activation energy term (E) and thermophoresis Nt as well as brownian motion Nb terms.
• The nanoparticle concentration boundary layer diminishes with growth in the Schmidt number and brownian motion terms but the reverse is the case for growth in the thermophoresis term Nt. • A dampen momentum boundary layer is encountered as the magnetic field term M rises but the thermal field increases with temperature ratio term and radiation terms develop.

References

[1]. Akbar, N. S., Nadeem, S., Haq R. U. and Khan, I. Radiation effects on MHD stagnation point flow of nano fluid towards a stretching surface with convective boundary condition, Chinese Journal of Aeronautics, 2013; 26(6): 1389-1397.
[2]. Akbar, N. S., Nadeem, S., Haq R. U. and Khan, M. Radiation effects on MHD stagnation point flow of nanofluid towards a stretching surface with convective boundary condition, Chinese Journal of Aeronautics, 2013; 26(6): 1389-1397.
[3]. Akinbobola, T. E. and Okoya, S. S. The flow of second grade fluid over a stretching sheet with variable thermal conductivity and viscosity in the presence of heat source/sink, Journal of the Nigerian Mathematical Society, 2015; 34: 331-342.
[4]. Ali, M. E. Heat transfer characteristics of a continuous stretching surface, Warme-und Stoffubertragung, 1994; 29(4): 227-234.
[5]. Attili, B. S. and Syam, M. L. Efficient shooting method for solving two point boundary value problems, Chaos, Solitons and Fractals, 2008; 35(5): 895-903.
[6]. Crane, L. J. Flow past a stretching plate, Communicatios Breves, 1970; 21: 645-647.
[7]. Eringen, A. C. Theory of micropolar fluids. J. Math. Anal. Appl., 1966; 16: 1-18.
[8]. Eringen, A. C. Theory of thermo-microfluids. Journal of Mathematical Analysis and Applications, 1972; 38: 480-496.
[9]. Das, K., Jana, S. and Kundu, P. K. Thermophoretic MHD slip flow over a permeable surface with variable fluid properties, Alexandria Engineering Journal, 2015; 54: 35-44.
[10]. Fatunmbi, E. O. and Fenuga, O. J. MHD

micropolar fluid flow over a permeable stretching sheet in the presence of variable viscosity and thermal conductivity with Soret and Dufour effects. International Journal of Mathematical Analysis and Optimization: Theory and Applications, 2017: 211- 232.

[11]. Fatunmbi, E. O. and Adeniyan, A. MHD stagnation point-flow of micropolar fluid past a permeable stretching plate in porous media with thermal radiation, chemical reaction and viscous dissipation. Journal of Advances in Mathematics and Comp Science, 2018; 26(1): 1-19.

[12]. Khan, M. I., Hayat, T., Khan, M. I. and Alsaedi, A. Activation energy impact in nonlinear radiative stagnation point flow of cross nanofluid, International Communications in Heat and Mass Transfer, 2018; 91: 216-224.

[13]. Kumar, L. Finite element analysis of combined heat and mass transfer in hydromagnetic micropolar flow along a stretching sheet. Comput Mater Sci, 2009; 46: 841-848. Doi:10.1371/journal.pone.0059393

[14]. Kumar, R. V. M. S. S. K., Kumar, G. V., Raju, C. S. K., Shehzad, S. A. and Varma, S. V. K.J. (2018). Analysis of Arrhenius activation energy in magnetohydrodynamic Carreau fluid flow through improved theory of heat diffusion and binary chemical reaction, Phys. Commun. 2018; 2: 1-15.

[15]. Lukaszewicz, G. *Micropolar fluids: Theory and Applications* (1st Ed.). Birkhauser,Boston. 1999

[16]. Mabood, F., Ibrahim, S. M. and Khan, W. A. Effect of melting and heat generation/absorption on Sisko nanofluid over a stretching surface with nonlinear radiation. Physica Scripta, 2019; 94 (6): 065701.

[17]. Makinde, O. D. and Aziz, A. Boundary layer flow of a nanofluid past a stretching sheet with a convective boundary condition. *International Journal of Thermal Sciences,2011; 50*: 1326-1332.

[18]. Mahanthesh, B., Gireesha, B. J., Gorla, R. S. R. and Makinde ,O. D. Magnetohydrodynamic three-dimensional flow of nanofluids with slip and thermal radiation over a nonlinear stretching sheet: a numerical study, Neural Computing and Applications, 2018; 30(5): 1557-1567.

[19]. Mabood, F. and Das, K. Melting heat transfer on hydromagnetic flow of a nanofluid over a stretching sheet with radiation and second order slip, Eur. Phys. J. Plus 2016; 131(3).

[20]. Noor, N. F. M., Haq, R. U., Nadeem, S. and Hashim, I. Mixed convection stagnation flow of a micropolar nanofluid along a vertically stretching surface with slip effects, Meccanica, 2015, 1-16.

[21]. Parida, S. K., Panda, S. Rout, B. R. (2015). MHD boundary layer slip flow and radiative

[22]. nonlinear heat transfer over a flat plate with variable fluid properties and thermophoresis, Alexandria Engineering Journal, 2015; 54: 941-953.

[23]. Qasim, M., Khan, I. and Shafle, S. Heat transfer in a micropolar fluid over a stretching sheet with Newtonian heating. *Plos One, 2013; 8*(4): 1-6.

[24]. Ramzan, M, Ullah, N., Chung, J. D., Lu, D. and Farooq, U. Buoyancy effects on the radiative magneto micropolar nanofluid flow with double stratification, activation energy and binary chemical reaction, Scientific Reports, 2018; 7: 1-15.

[25]. Reena and Rana, U. S. Effect of Dust Particles on rotating micropolar fluid heated from below saturating a porous medium. Applications and Applied Mathematics: An International Journal, 2009; 4: 189-217.

[26]. Vajravelu, K. Viscous flow over a nonlinearly stretching sheet., Appl. Math. Comput., 2001; 124: 281-288.

[27]. Xu, L. and Lee, E.W.M. Variational iteration method for the magnetohydrodynamic flow over a nonlinear stretching sheet. Abst Appl Anal 5 pages (2013).

7/22/2023